Electronic Supplementary Information

Chiral organic-inorganic hybrid perovskites synthesized using acoustofluidic closed system

Tao Zhou[a], Yan Yu[a], Haonan Zhang[a], Chong Li[a, b], Ran Tao[a *], Fujian Ren[c], Chen Fu[a], Jingting Luo[a], Yongqing Fu[d]

a *Shenzhen Key Laboratory of Advanced Thin Films and Applications, College of Physics and Optoelectronic Engineering, Shenzhen University, Shenzhen 518060, China*
b School of Electronic Engineering, Huainan Normal University, Huainan, 232038, China.
c Advanced Materials Laboratory, School of Materials Science and Engineering, Tsinghua University, Beijing 100084, China
d Faculty of Engineering and Environment, Northumbria University, Newcastle upon Tyne NE1 8ST, UK

Calculation

The direct energy band gap ($(Ahv)^2$) was calculated using the following equation:

$$(Ahv)^2 = (Absorbance \times \frac{1240}{wavelength})^2$$

The anisotropy factor g_{CD} was calculated using the following equation:

$$g_{CD} = \frac{CD[mdeg]}{32980 \times Absorption}$$

The various data from the above tests on OIHPs were visualized using the software ORIGIN.

The flow rate assessment is conducted through the analysis of particle motion as recorded by a high-speed camera. During a single experimental trial, ImageJ is employed to monitor the trajectories of five distinct

particles. The time intervals are established according to the number of frames captured, and subsequently, an average is calculated to derive the flow rate.

The membrane thickness is determined by calculating the difference between the average height of the grooves and the average height of the entire scanned field of view, as measured by the profilometer. Both the overall average height and the average height of the grooves are computed using the software Gwyddion.

Concentration Consumption Assessment

Within the SAWM system, film deposition occurs within a sealed reaction chamber. To evaluate concentration fluctuations of the precursor solution during the coating process, we performed a quantitative analysis of solute consumption. Specifically, a reaction chamber containing a 30 wt% precursor solution displayed a mass increment of 321.6 mg, equivalent to a total solute mass of 96.48 mg. Subsequent to three consecutive film depositions, the target substrate exhibited mass gains of 0.47 mg, 0.42 mg, and 0.63 mg, respectively. Based solely on solute depletion, the calculated concentration variation ranges from 0.44% to 0.65%. Considering the concurrent evaporative loss of solvent during the annealing stage, the actual concentration consumption is anticipated to be even less. Consequently, we posit that the influence of precursor solution concentration changes on the film deposition process is negligible.

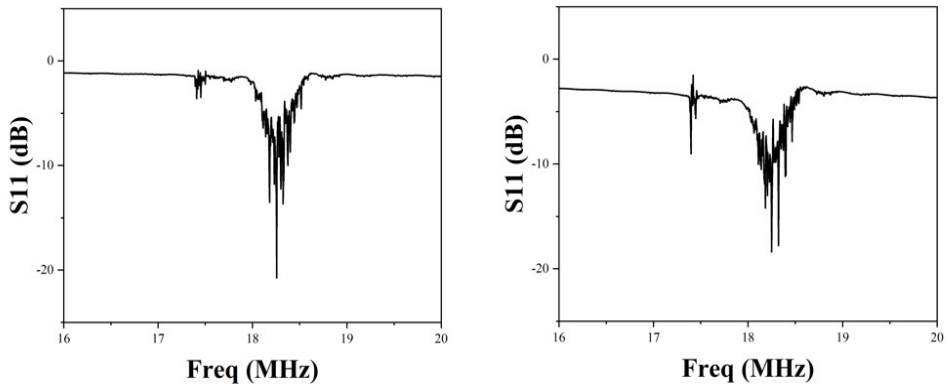

Figure. S1 Reflection spectrum (S11) of two IDTs with a misalignment of 0.5 and a wavelength of 200 μm, a -20 dB return loss demonstrates the high efficiency of the SAW device.

Definition

Fig. S1 is a top view schematic of the SAW device. The wavelength of IDT is measured at 200 μm. Each cycle comprises two fingers and two gaps, with both the width of the fingers and the gaps being 50 μm. Additionally, there exists a misalignment of 0.5 on either side of the IDT, where misalignment is defined as:

$$misalignment = \frac{Acoustic\ aperture - lap\ length}{Acoustic\ aperture}$$

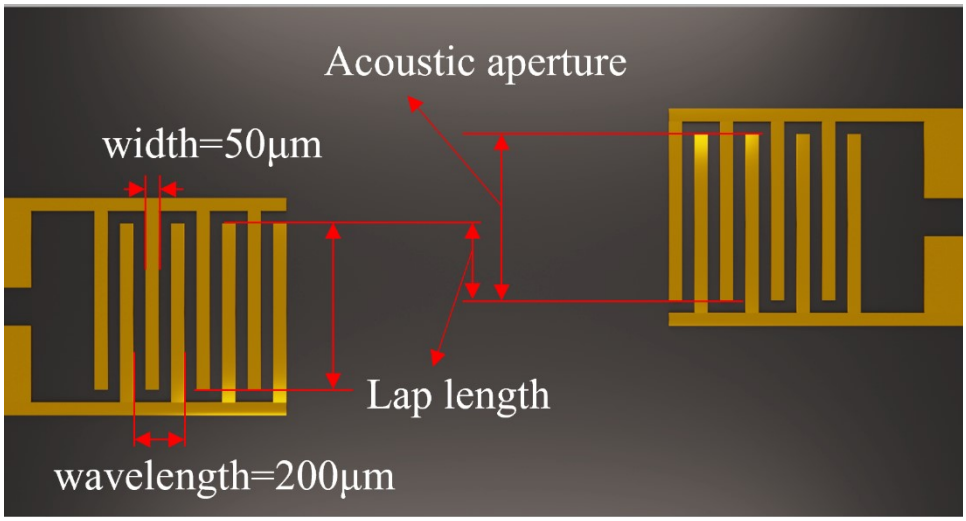

Figure. S2 Top view schematic of the SAW device shows a wavelength of 200 μm, with both the width of the fingers and the gaps measuring 50 μm each. The acoustic aperture refers to the extent of the overlapping sections of the fingers on either side of a single IDT, while the overlap length denotes the overlapping length of the functional components of two IDTs.

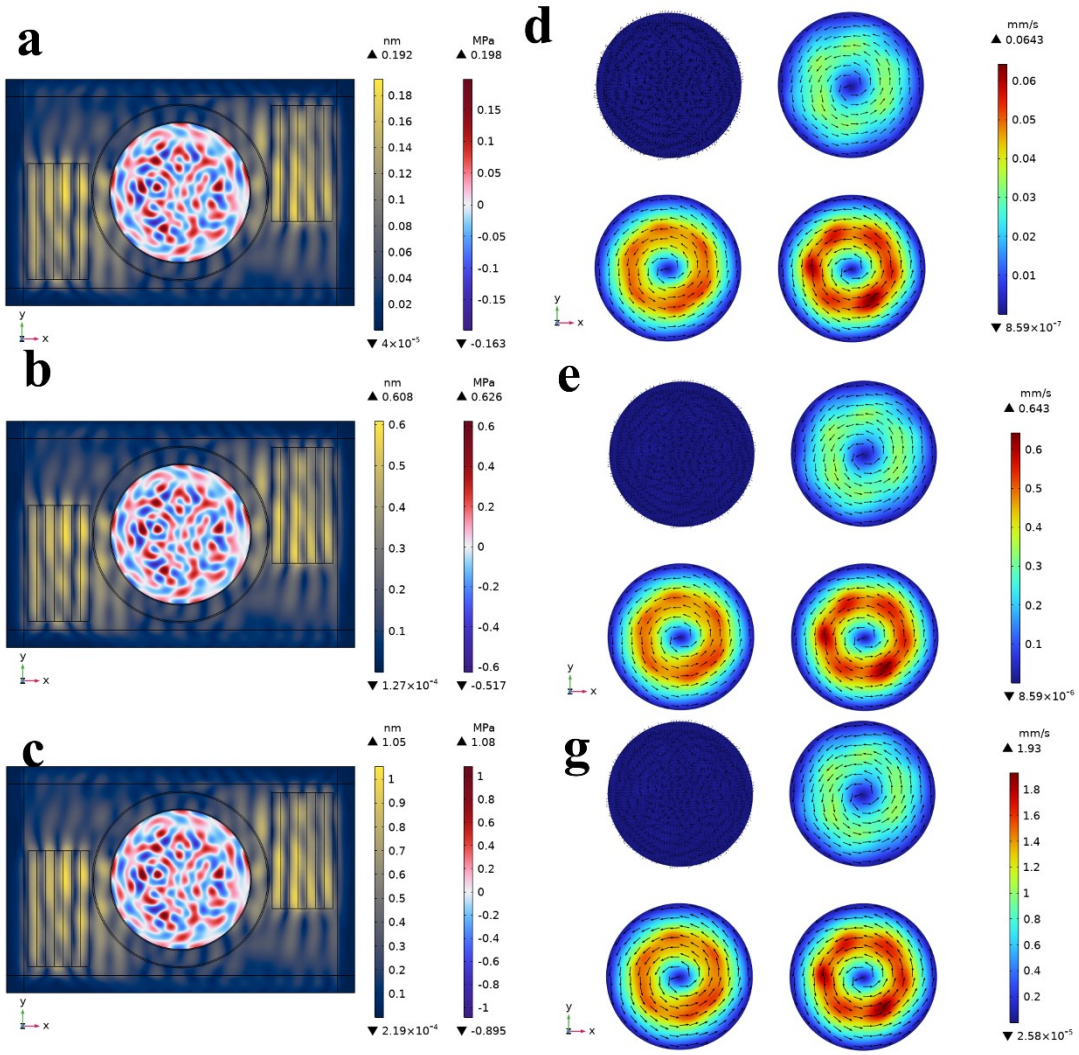

Figure. S3 The surface displacement of IDT and the distribution of the acoustic radiation field in the reaction cell are observed at power levels of (a) 0.1 W, (b) 1 W, and (c) 3 W. Additionally, the distribution of the flow velocity field is analyzed at the bottom of the reaction cell, at 1/3 height, 2/3 height, and at the liquid surface for power levels of (d) 0.1 W, (e) 1 W, and (f) 3 W, respectively.

Repeatability and Reproducibility Assessment

The repeatability and reproducibility of the SAWM system were evaluated through three consecutive film depositions under consistent operational parameters: 2 W input power, 30 wt% precursor solution, and a 10-minute coating. SEM results (Fig. S4) revealed high similarity in surface morphology and consistent crystal dimensions across all three samples. Furthermore, film thickness and Ra measurements (Tab. S1), conducted at multiple locations on each sample, demonstrated minimal variation, with fluctuations within a 0.2 μm range, thereby confirming the repeatable and reproducible nature of the SAWM system.

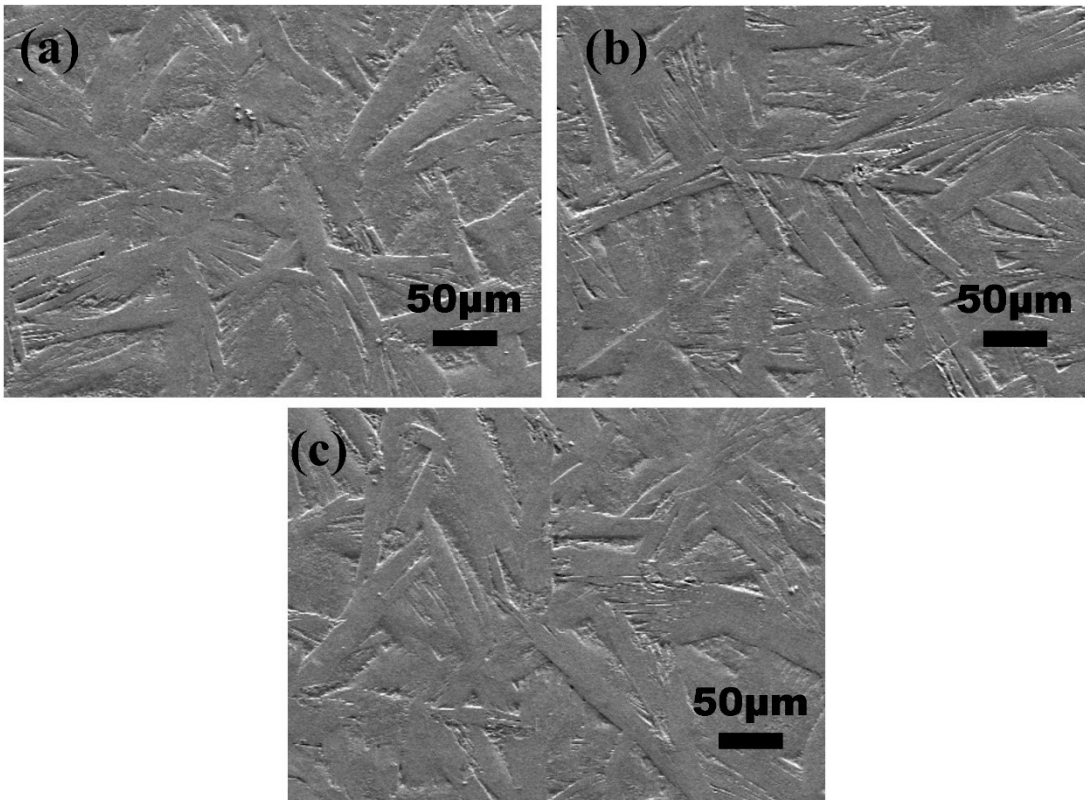

Figure.S4 SEM images of (a) the first, (b) second, and (c) third consecutive SAW-coated films

Table. S1 Thickness and Ra data for different regions of three repeated samples

Samples	Sample 1			Sample 1			Sample 1		
Tests	1	2	3	1	2	3	1	2	3
Thickness (μm)	1.42	1.57	1.65	1.62	1.71	1.54	1.54	1.39	1.61
Ra (μm)	0.61	0.68	0.55	0.71	0.64	0.73	0.67	0.57	0.63

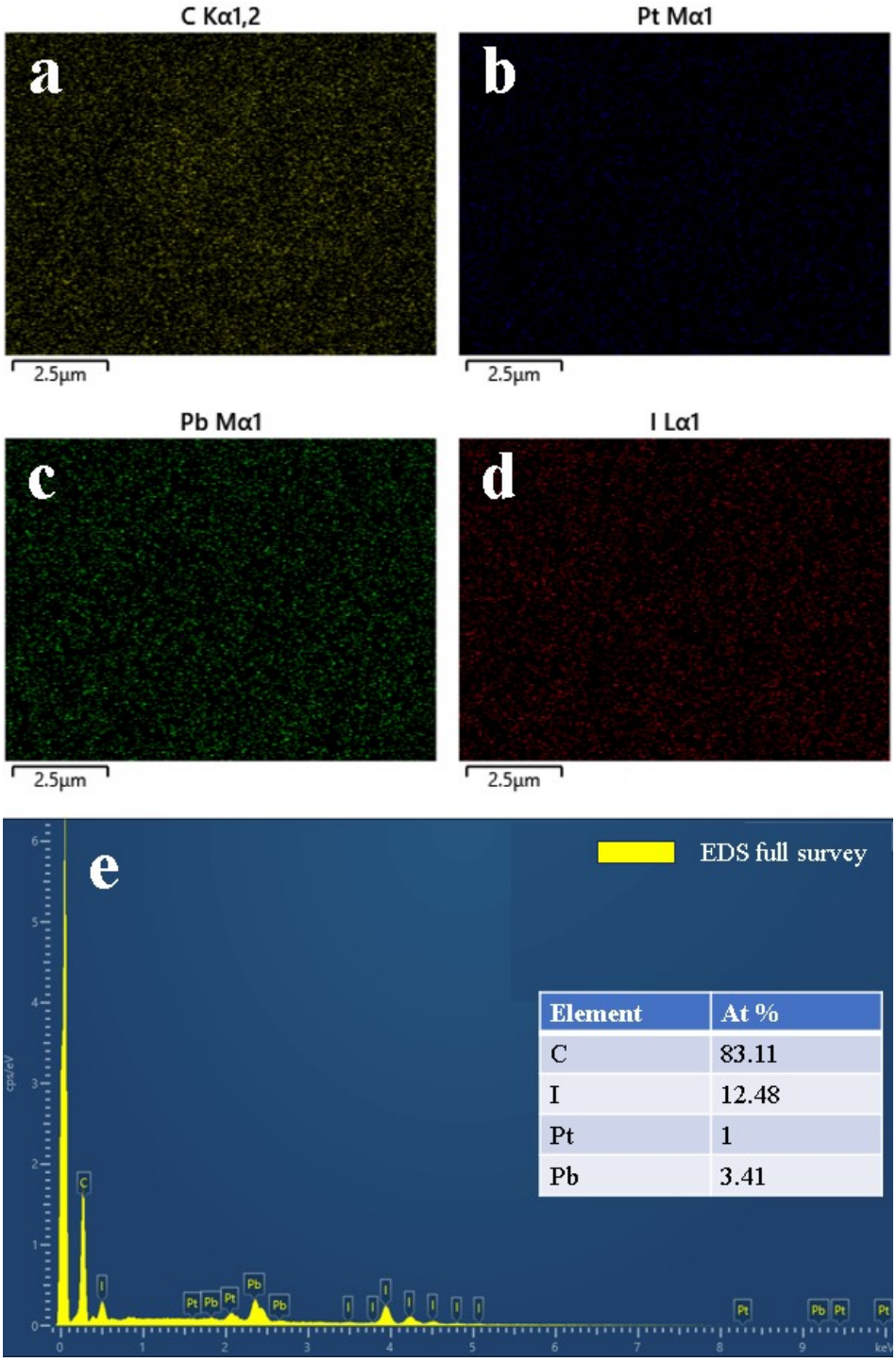

Figure.S5 The dispersion of the elements a) C, b) Pt, c) Pb, and d) I in 30 wt% SAW film, as well as the e) EDS full survey with atomic ratios.

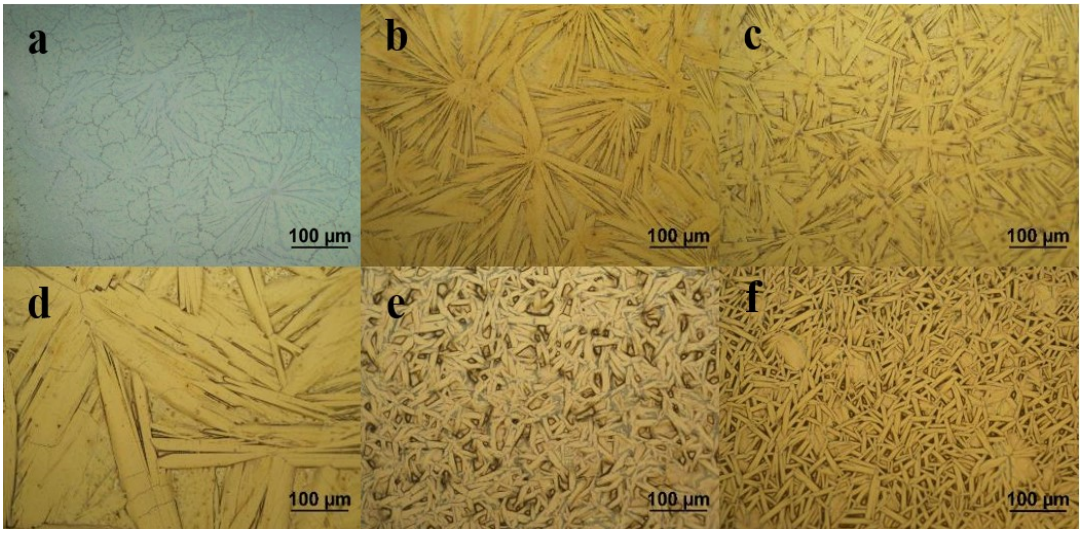

Figure.S6 The topography of S-Chiral SAW films was synthesized using solutions with concentrations of a) 5 wt%, b) 10 wt%, c) 20 wt%, d) 30 wt%, and e) 50 wt%, driven at 2 W power for 10 minutes. The f) surface morphology of a 30 wt% film when the drive time was increased to 20 minutes.

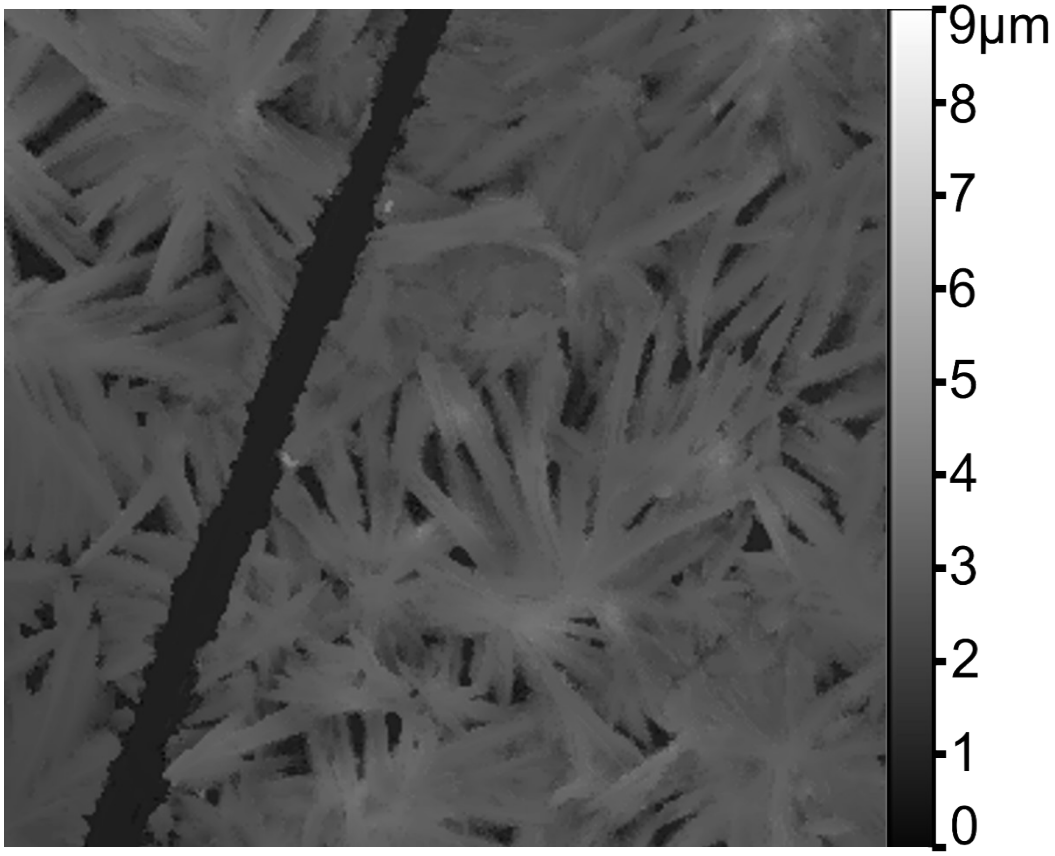

Figure.S7 Thickness distribution of SAW coating films by profilometer，the film thickness is approximately 1.5 μm.

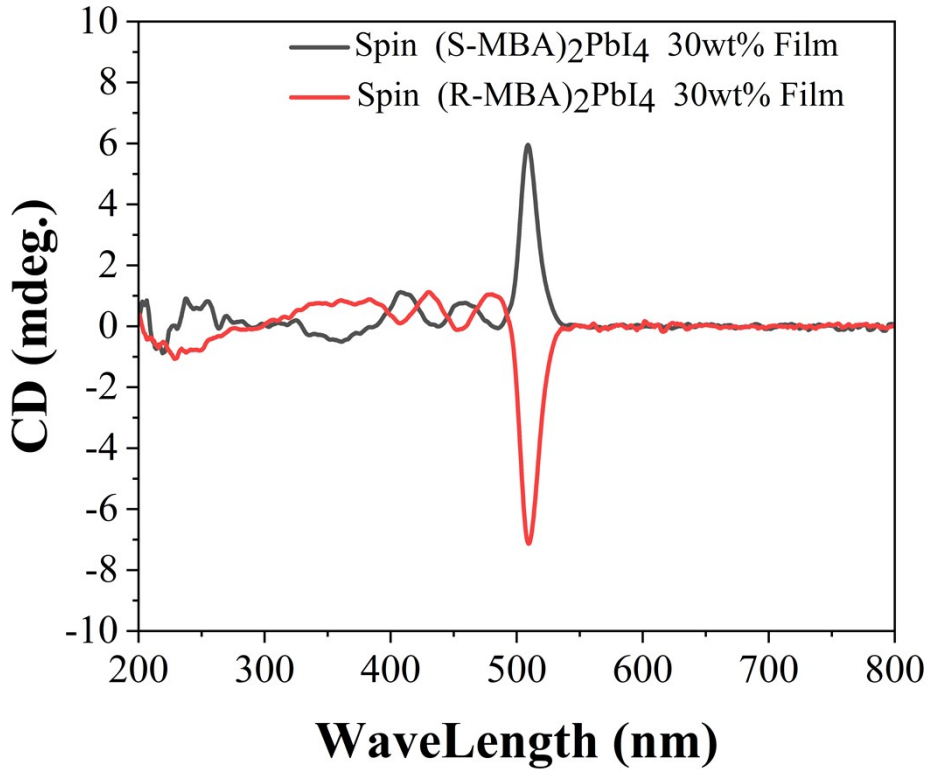

Figure.S8 The circular dichroism spectra of the Spin-coated films.

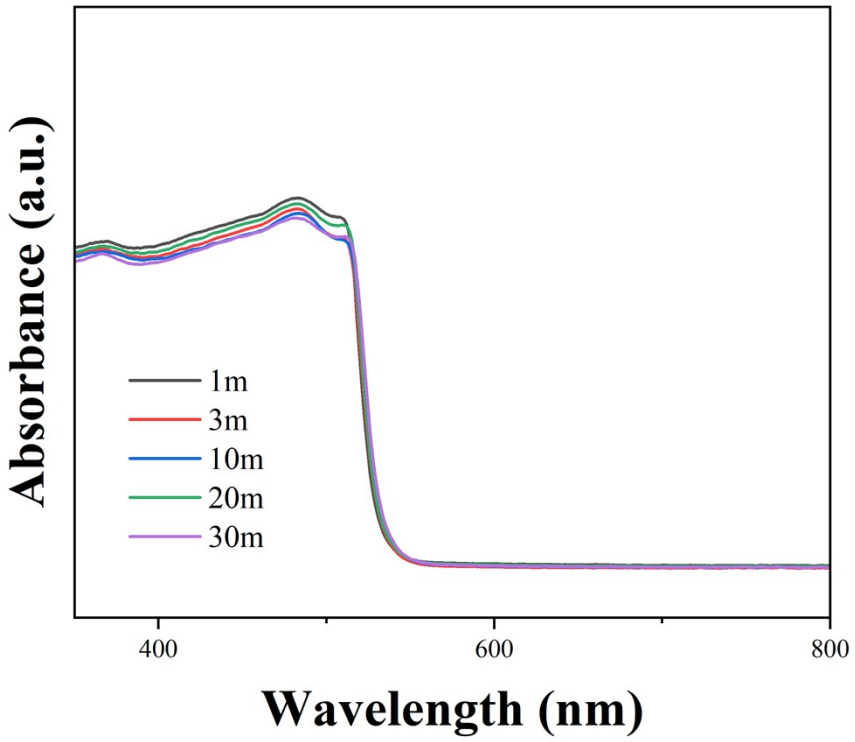

Figure.S9 Absorbance of SAW films in driving time of 1，3，10，20，30 minutes

Video.S1 Vortices within the SAWM system were recorded using a high-speed camera at 0.1W input.

Video.S2 Vortices within the SAWM system were recorded using a high-speed camera at 0.4W input.

Video.S3 Vortices within the SAWM system were recorded using a high-speed camera at 4W input.

Video.S4 Vortices within the SAWM system were recorded using a high-speed camera at 10W input.